

DEVP, B' = DMVP and DPVP) on the basis of their intrinsic coordination strength to each other (DAVP > 2VP).¹⁴

After dissolving the calculated amount of catalyst in dichloromethane, the respective equivalents of 2VP were added in one portion. The polymerization is quantitative after a short period of time (90 min) at room temperature. Before addition of monomer B (and B') an aliquot sample is taken from the solution and quenched by the addition of CD₃OD (calculation of conversion of 2-vinylpyridine *via* ¹H-NMR and for GPC analysis). The advantage of GTP compared to other polymerization types is the synthesis of homopolymer with an exact adjustable mass and a very low polydispersity. The monomer addition for the vinylphosphonates (BB'-random-copolymer) is achieved through simple pre-addition mixing of DEVP and DMVP/DPVP and subsequent addition to the reaction mixture making GTP a suitable method for generating blockcopolymers effortlessly. The desired block copolymers were isolated through precipitation from *n*-pentane. All polymer samples show atactic microstructures, monomodal distributions and very narrow molecular weight distributions ($D < 1.15$) (Table 1). As a benefit, no fraction of P2VP-homopolymer is observed in the blockcopolymer as found for anionic polymerization when performing blockcopolymerizations with P2VP.¹⁷ In addition, no homopolymer of PDAVP is formed due to an initiator efficiency of 99% for catalyst 1 for the 2VP polymerization avoiding unreacted catalyst in the reaction mixture.¹² This advantage is of great interest for drug delivery systems leading to unimodal blockcopolymers all with the same composition to form identical micelles without further purification of the polymers. Molecular-weights and molecular-weight distributions of block A is measured *via* GPC-MALS analysis of the first aliquot. The molecular-weight of the blockcopolymer is determined through the ratio of A/B and the molecular weight of the first block (A). Composition A/B [2VP/DAVP] is calculated *via* ¹H-NMR-spectroscopy of the dried blockcopolymer. For AB polymers the CH₂-signal of the phosphate-ester is compared with an aromatic proton of the P2VP-side chain (Fig. S7†). For ABB'

polymers the combined CH₃-signals of the phosphate-esters are used (Fig. 2). Blockcopolymers with a monomer feed of A/B 1 : 1 all show a similar ratio of A/B in the polymer regardless of whether AB or ABB' blockcopolymers are obtained (A/B = 1/0.7–1/0.8; Table 1, entry 1, 2, 5–7). In all blockcopolymers, roughly 80% of the respective dialkylvinylphosphonate is converted and incorporated in the polymer chain, independent from the used amount of monomer. For the composition of B/B' [DEVP/DPVP, DMVP] in case of PDMVP A(BB')² the proportion of PDEVP and PDMVP-signals in the ³¹P-NMR-spectrum can be used, as the calculation is consistent both for calculation *via* ¹H-NMR and *via* ³¹P-NMR-spectra. Due to overlapping of PDEVP and PDPVP-³¹P-signals, the composition in A(BB')¹ is calculated solely *via* ¹H-NMR-spectroscopy of the CH₃-signals (Fig. 2).¹⁵ Due to a perfect regulation of the polymer composition by the monomer feed, it is possible to incorporate only small amounts of DPVP/DMVP in the ABB' polymers. For A(BB')¹ 5% of block B consists of DPVP. Almost 10% of DMVP is contained in blockcopolymer A(BB')². The obtained amphiphilic polymers have a critical micelle concentration (CMC) above which they self-assemble to micelle structures. The CMC was determined by a dialysis method using Nile red, a water insoluble and fluorescent dye and was found to be at 0.13 mg mL⁻¹ (Fig. 3). In general, a lower CMC is observed for polymeric micelles in contrast to other surfactants (*ca.* 4–10 mg mL⁻¹) leading to a higher thermodynamic stability of the system.^{18,19} TEM measurements image the unimodal size distribution of these polymers (Fig. 3). Because the hydrophilic chain is longer or the same as the hydrophobic one, core-shell-type spherical micelles are observed, in which the hydrophobic core (P2VP) is shielded from the aqueous milieu by the hydrophilic segments (PDAVP). For the application of micelles in the human body a diameter of 10–100 nm is necessary, which is near to other natural vehicles, to avoid renal excretion and filtration and to ensure the cellular uptake without the recognition by the immune system.^{16,18–20}

Via REM-GTP it is possible to exactly tune the composition of the micelle structure through the monomer feed. Different feed

Table 1 AB and ABB'-block copolymers with different compositions produced with catalyst 1

Entry	Polymer	Feed ^a A _{eq} /B _{eq}	Composition A/B ^b [2VP/DEVP]	M _n (A) × 10 ^{4c} [g mol ⁻¹]	M(AB) _{n,NMR} × 10 ^{4d} [g mol ⁻¹]	D ^e	LCST (H ₂ O) ^f [°C]	D _h ^g [nm]
1	AB ¹	2VP ₁₀₀ /DEVP ₁₀₀	1/0.8	2.5	5.6	1.06	43.5	46 ± 3
2	AB ²	2VP ₅₀ /DEVP ₅₀	1/0.8	1.3	2.9	1.04	—	—
3	AB ³	2VP ₅₀ /DEVP ₉₀	1/1.5	1.3	4.5	1.09	43.5	40 ± 5
4	AB ⁴	2VP ₅₀ /DEVP ₁₂₀	1/1.9	0.9	3.6	1.15	43.0	48 ± 4
5	AB ⁵	2VP ₂₀₀ /DEVP ₂₀₀	1/0.8	4.1	9.3	1.05	43.0	156 ± 16
Entry	Polymer	Feed ^a A _{eq} /B _{eq} /B' _{eq}	Composition A/BB' ^b [2VP/DAVP]	M _n (A) × 10 ^{4c} [g mol ⁻¹]	M(ABB') _{n,NMR} × 10 ^{4d} [g mol ⁻¹]	D ^e	LCST (H ₂ O) ^f [°C]	D _h ^g [nm]
6	A(BB') ¹	2VP ₁₀₀ /DEVP ₉₇ /DPVP ₃	1/0.8	2.4	4.8	1.07	38.5	62 ± 5
7	A(BB') ²	2VP ₁₀₀ /DEVP ₉₀ /DMVP ₁₀	1/0.7	2.0	3.7	1.05	48.5	48 ± 4

^a By weighing the monomer, [M]/[cat.] = eq., [cat.] = 41.7 μmol in 2.5 mL CH₂Cl₂. ^b Calculated from ¹H NMR spectroscopy. ^c Determined by GPC-MALS (M_w/M_n of the blockcopolymers). ^d Determined by ¹H NMR spectroscopy. ^e Polydispersity index. ^f Determined by temperature dependent UV/VIS measurements at transmittance decrease of 10%. ^g Measured by DLS. The micelle size is given as the average hydrodynamic diameter.



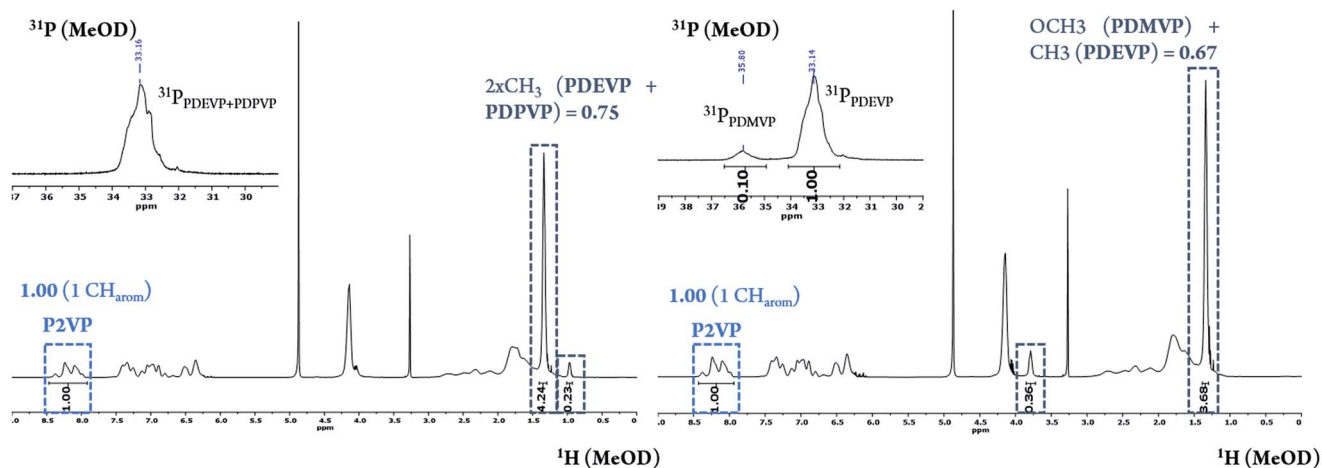


Fig. 2 ^1H - and ^{31}P -NMR spectrum of AB^1 ($2\text{VP}_{100}/\text{DEVP}_{97}/\text{DPVP}_3$; Table 1, entry 6, left) and AB^2 ($2\text{VP}_{100}/\text{DEVP}_{90}/\text{DMVP}_{10}$; Table 1; entry 7; right) in MeOD at 298 K. Assignment of the protons according to Rieger *et al.* overlapping of PDEVP and PDPVP- ^{31}P -signal.¹⁵

compositions were set to vary the chain length of the hydrophobic P2VP block and also the hydrophilic PDEVP block length was changed to analyze the differences in micelle formation (Table 1). The size of the micelles was determined by dynamic light scattering (DLS).

The measurements of all synthesized polymers (Table 1, entry 1–7) show that a minimum P2VP and PDEVP length is required to sustain the micelle formation in H_2O . At 2.5 wt%, fifty repeating units of 2VP and DEVP did not suffice for the formation of stable micelles in water (Table 1, entry 2). Upon increasing the chain length to 100/100 ratio between P2VP and PDEVP stable and perfectly sized (~ 50 nm) micelles can be observed (Table 1, entry 1).

The DLS-measurements underline the unimodal shape and the narrow size distribution of the AB-polymer (Fig. 3). Further increased chain length to 200/200 (P2VP/PDEVP, Table 1, entry 5) also resulted in stable micelles, but gave micelles with diameters of >100 nm and are therefore not suitable for targeting approaches. Whereas P2VP is insoluble in water under neutral conditions, a decrease of the pH-value to 5 in P2VP-PEO vehicles led to a protonation of the P2VP-block and in consequence to a dissociation of the membrane with subsequent

release of the encapsulated substance.²¹ These systems can be used for applications in drug delivery, because some cellular compartments (*e.g.* endosomal vesicles) show lower pH-values (5–6) than the one of normal blood (7.4). The pH-value is also effected by diseases as tumour cells are more acidic (pH \approx 6.5).^{18,20}

The pH-dependent solubility of our systems was investigated by titration with 0.1 M hydrogenchloride solution (Fig. S11†). The titration curve shows a high decrease to pH-value 4.5 after adding small amounts of HCl. In consequence, stable micelles are present at pH > 4.5 . This value of pH = 4.5 for dissolution of a P2VP-blockcopolymer is in agreement with other P2VP containing micelles where the dissolution occurs between pH = 4 and 5.^{17,21–23} To obtain multiresponsive micelles that are controllable not only *via* the pH-value, but also by temperature vinylphosphonates were introduced into the polymer. The suitability of phosphorous containing polymers for medical applications is well known, because of their high water solubility, thermal stability and non-toxicity.^{15,24} Therefore we performed temperature-dependent LCST-DLS measurements to show the reversible formation of micelles under hyperthermia. Below the LCST polymeric micelles are observed. When the

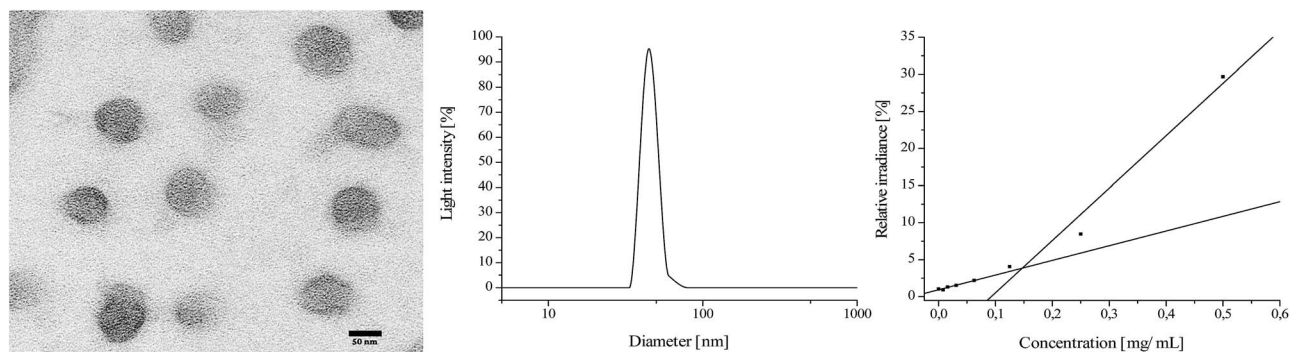


Fig. 3 Left: TEM-image of micelles from AB^1 (preparation see ESI†). Middle: dynamic light-scattering of micelles from AB^1 (2.5 mg mL^{-1}) in H_2O . Right: determination of critical micelle concentration (CMC) with Nile red. All figures for AB^1 ($2\text{VP}_{100}/\text{DEVP}_{100}$; Table 1, entry 1).



temperature is above the LCST a loaded drug can be released due to aggregation of the polymer. In the human body the drug would be released *e.g.* by a hyperthermic stimuli to the disease area.²⁰ The cloud points of PDEVP homopolymers (230 kg mol⁻¹) was found to remain constant at low concentrations (0.1–2.5 wt%; 42 °C), but increases to 71 °C at high concentrations 67 wt%.^{15,25} The influence of P2VP on the LCST and the limits of adequate vinylphosphonate content within the polymer was tested in this study. These thermoresponsive measurements of the AB blockcopolymers (2.5 wt%) in H₂O show that the presence of P2VP and also the variation of chain length of PDEVP (ratio: P2VP/PDEVP 1/0.8–2.0; Table 1) have no measureable effect on the cloud points (43–43.5 °C) under the evaluated conditions. This is remarkable and can be used as an advantage over other thermoresponsive copolymers (poly-*N*-isopropylacrylamide (PNIPAm) or polyethyleneglycol (PEG)) as they show a significant influence of both, hydrophilic and hydrophobic, blocks on their LCST-behaviour.^{26,27} The independence of the LCST in P2VP-PDAVP polymers on the chain lengths and the P2VP-block in our study allows higher variation possibilities regarding the hydrophilic and hydrophobic chain segment as well as a better predictability and adjustability of the LCST. To test the influence of salts and buffer solutions on the LCST the cloud point of AB¹ was measured in PBS (phosphate buffered saline) (Fig. S13[†]). Due to a salting-out effect of the phosphate salt in PBS, which leads to a dehydration of the polymers, a decrease in the LCST of about 4 °C is observable. This decrease is lower than the ones of other stimuli responsive polymers *e.g.* PEG or PNIPAm resulting in a better applicability of our novel micelles in biomedical usage due to a lower impact of environmental conditions.^{15,28}

As a drawback, a release temperature of 44 °C which must be used for this micelles with an LCST at around 43 °C is not in the normal body temperature range which is between 36.2 and 37.5 °C.²⁹ Therefore our investigation was directed to the evaluation of ABB' blockcopolymers to proof the suitability of vinylphosphonates as substrates to tune the LCST in micellar

systems within a physiologically relevant temperature range for potential medical application. The introduction of small amounts of DMVP or DPVP (3–10 eq.) statistically incorporated into the DEVP block has distinct influence and makes it possible to shift the cloud point of the copolymers (Fig. 4). The incorporation of at least 10 equivalents of hydrophobic DMVP suffice to increase the LCST up to 48.5 °C, while maintaining perfect control of the micellar architecture and without affecting the hysteresis upon cooling (Table 1, entry 7). Likewise, DPVP (even only 3 eq.) with its hydrophilic properties successfully decreases the LCST of ABB' block copolymers to 38.5 °C (Table 1, entry 6). For application in drug delivery a temperature of around 39 °C can be used which is near the normal body temperature range.

Conclusions

In summary, AB-blockcopolymers from 2VP and DAVP can be produced *via* REM-GTP with narrow molecular weight distribution and precise molecular-weight through variation of the monomer feed. These tailor-made blockcopolymers self-assemble into unimodal micelles at a low CMC, indicating a high thermodynamic stability. This stability in combination with the multiresponsive amphiphilic properties (pH-dependent solubility and LCST) of the micelles, which are investigated for the first time, making them adequate for targeting approaches. These micelles show several advantages over other micelle systems in matters of precise synthesis and exact control over the micelle structure. To use the lower critical solution temperature for release in the human body, the LCST has to be tuned to the physiologically relevant temperature range. In our study we showed, that only the vinylphosphonate block has influence on the thermoresponsive behaviour and can selectively be utilized to tune the LCST through the monomer feed. The observed a-P2VP-b_{random}-(PDEVP-co-PDMVP/PDPVP)-polymers in which small amounts of DMVP or DPVP are incorporated into the polymer chain shift the LCST of the micelles. Hydrophobic DMVP increases the LCST, whereas DPVP with its hydrophilic properties successfully decreases the LCST by maintaining perfect micelle structures. The possibility to tune the micelle structure *via* monomer feed, to generate desired properties, opens a new field for the application of amphiphilic micelles.

Acknowledgements

F. Adams thanks the Bavarian State Ministry of Environment and Consumer Protection for financial support within BayBio-tech research network. The authors thank Dr Marianne Hanzlik for the TEM measurements.

Notes and references

- 1 B. S. Soller, S. Salzinger and B. Rieger, *Chem. Rev.*, 2016, **116**, 1993–2022.
- 2 B. S. Soller, N. Zhang and B. Rieger, *Macromol. Chem. Phys.*, 2014, **215**, 1946–1962.

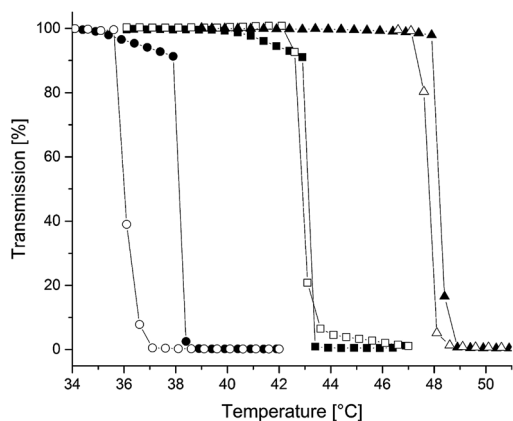


Fig. 4 Determination of the cloud points of AB (squares), A(BB')¹ (circles) and A(BB')² (triangles) block copolymers. The cloud point was determined at 10% decrease of transmittance for 2.5 wt% aqueous polymer solution.



- 3 E. Y. X. Chen, *Chem. Rev.*, 2009, **109**, 5157–5214.
- 4 H. Yasuda, M. Furo, H. Yamamoto, A. Nakamura, S. Miyake and N. Kibino, *Macromolecules*, 1992, **25**, 5115–5116.
- 5 E. Ihara, M. Morimoto and H. Yasuda, *Macromolecules*, 1995, **28**, 7886–7892.
- 6 B. S. Soller, Q. Sun, S. Salzinger, C. Jandl, A. Pöthig and B. Rieger, *Macromolecules*, 2016, **49**, 1582–1589.
- 7 B. S. Soller, S. Salzinger, C. Jandl, A. Pöthig and B. Rieger, *Organometallics*, 2015, **34**, 2703–2706.
- 8 S. Salzinger, B. S. Soller, A. Plikhta, U. B. Seemann, E. Herdtweck and B. Rieger, *J. Am. Chem. Soc.*, 2013, **135**, 13030–13040.
- 9 U. B. Seemann, J. E. Dengler and B. Rieger, *Angew. Chem., Int. Ed.*, 2010, **49**, 3489–3491.
- 10 P. T. Altenbuchner, F. Adams, A. Kronast, E. Herdtweck, A. Pöthig and B. Rieger, *Polym. Chem.*, 2015, **6**, 6796–6801.
- 11 J. F. Carpentier, *Organometallics*, 2015, **34**, 4175–4189.
- 12 P. T. Altenbuchner, B. S. Soller, S. Kissling, T. Bachmann, A. Kronast, S. I. Vagin and B. Rieger, *Macromolecules*, 2014, **47**, 7742–7749.
- 13 C.-X. Cai, L. Toupet, C. W. Lehmann and J.-F. Carpentier, *J. Organomet. Chem.*, 2003, **683**, 131–136.
- 14 N. Zhang, S. Salzinger, B. S. Soller and B. Rieger, *J. Am. Chem. Soc.*, 2013, **135**, 8810–8813.
- 15 N. Zhang, S. Salzinger and B. Rieger, *Macromolecules*, 2012, **45**, 9751–9758.
- 16 K. Kataoka, A. Harada and Y. Nagasaki, *Adv. Drug Delivery Rev.*, 2001, **47**, 113–131.
- 17 T. J. Martin, K. Procházka, P. Munk and S. E. Webber, *Macromolecules*, 1996, **29**, 6071–6073.
- 18 G. Gaucher, M.-H. Dufresne, V. P. Sant, N. Kang, D. Maysinger and J.-C. Leroux, *J. Controlled Release*, 2005, **109**, 169–188.
- 19 R. J. Stokes and D. F. Evans, *Fundamentals of Interfacial Engineering*, WILEY-VCH, 1997.
- 20 S. Ganta, H. Devalapally, A. Shahiwala and M. Amiji, *J. Controlled Release*, 2008, **126**, 187–204.
- 21 U. Borchert, U. Lipprandt, M. Bilang, A. Kimpfler, A. Rank, R. Peschka-Süss, R. Schubert, P. Lindner and S. Förster, *Langmuir*, 2006, **22**, 5843–5847.
- 22 C. Tsitsilianis, D. Voulgaris, M. Štěpánek, K. Podhájecká, K. Procházka, Z. Tuzar and W. Brown, *Langmuir*, 2000, **16**, 6868–6876.
- 23 L. I. Atanase and G. Riess, *J. Colloid Interface Sci.*, 2013, **395**, 190–197.
- 24 G. David, C. Boyer, R. Tayouo, S. Seabrook, B. Ameduri, B. Boutevin, G. Woodward and M. Destarac, *Macromol. Chem. Phys.*, 2008, **209**, 75–83.
- 25 S. Salzinger, U. B. Seemann, A. Plikhta and B. Rieger, *Macromolecules*, 2011, **44**, 5920–5927.
- 26 X. Zhao, W. Liu, D. Chen, X. Lin and W. W. Lu, *Macromol. Chem. Phys.*, 2007, **208**, 1773–1781.
- 27 Y. Yu, D. Hong, Z. Liu, F. Jia, Y. Zhou and C. Leng, *J. Polym. Res.*, 2013, **20**, 1–8.
- 28 J.-F. Lutz, Ö. Akdemir and A. Hoth, *J. Am. Chem. Soc.*, 2006, **128**, 13046–13047.
- 29 M. Sund-Levander, C. Forsberg and L. K. Wahren, *Scandinavian Journal of Caring Sciences*, 2002, **16**, 122–128.

